Heliyon 11 (2025) e41526

Contents lists available at ScienceDirect

Heliyon

journal homepage: www.cell.com/heliyon

Research article

A family of coexisting multi-scroll chaos and its selected control in coupled non-oscillatory neurons: A case study

Bertrand Frederick Boui A Boya [a,b,*], Zeric Tabekoueng Njitacke [c], Adelaide Nicole Kengnou Telem [c], Jacques Kengne [a]

[a] Unité de Recherche d'Automatique et d'Informatique Appliquée (UR-AIA), IUT-FV Bandjoun University of Dschang, P.O. Box 134, Bandjoun, Cameroon
[b] Institute of Computer Technology and Information Security, Engineering and Technological Academy, Southern Federal University, P.O. Box 347900, Taganrog, Russia
[c] Department of Electrical and Electronic Engineering, College of Technology (COT), University of Buea, P.O. Box 63, Buea, Cameroon

ARTICLE INFO

Keywords:
Hopfield inertial neurons
Coexisting multi-scroll chaos
Basins of attraction
Bursting oscillation
and multistability control

ABSTRACT

This study presents a family of coexisting multi-scroll chaos in a network of coupled non-oscillatory neurons. The dynamics of the system are analyzed using phase portraits, basins of attraction, time series, bifurcation diagrams, and spectra of Lyapunov exponents. The coexistence of multiple bifurcation diagrams leads to a complex pattern of multi-scroll formation, which is further complicated by the presence of coexisting single-scroll attractors that merge to form multi-scroll chaos. In addition, the presence of bursting phenomena and multiple firing partners is present in the model. A control strategy based on a noninvasive control method is applied to select the desired multi-scroll. The effectiveness of the control method is demonstrated through numerical simulations. The experimental validation on an Arduino microcontroller confirms the theoretical results and demonstrates the feasibility of implementing the proposed model. These remarkable behaviors hold significant implications for understanding brain dynamics and have potential applications in various fields.

1. Introduction

The intricate dynamics of the human brain, characterized by chaotic electrical signal transmission between neurons during cognitive processes and emotional expressions, have inspired research into neural networks and chaotic systems [1–3]. The unpredictability, ergodicity, and pseudo-randomness exhibited by chaotic neural networks present a unique avenue for exploration in complexity science. The complex topology of multi-scroll chaos offers high complexity and mirrors the brain's chaotic behavior. Multi-scroll chaos is a complex nonlinear dynamical behavior characterized by the presence of spiraling toward a distinct attractor in the phase space. The ability to produce multiple scrolls or chaotic trajectories makes these attractors particularly valuable for applications in secure communications, random number generation, and chaotic synchronization [4].

In recent years, numerous studies have revealed the presence of multi-scrolls in different systems/circuits with various methods. Bao et *al.,* [5] present a 2D non-autonomous neuron model with sinus activation functions, and multi-scroll chaotic attractors have

* Corresponding author. Institute of Computer Technology and Information Security, Engineering and Technological Academy, Southern Federal University, P.O. Box 347900, Taganrog, Russia.
E-mail address: bertrandboui22@yahoo.com (B.F. Boui A Boya).

https://doi.org/10.1016/j.heliyon.2024.e41526
Received 5 June 2024; Received in revised form 26 December 2024; Accepted 26 December 2024
Available online 27 December 2024

emerged with lines of equilibrium points. Parametric control of multi-scrolls has been shown using sine-piecewise-linear functions, revealing complex multi-scroll attractors [6,7]. Dana et *al.*, investigate a unidirectional coupling scheme of two chaotic oscillators with piecewise linear functions and reveal interesting multi-scroll dynamics without additional breakpoints [8]. Similarly, Monroy et *al.* [9], designed a chaotic system able to generate diverse multi-scroll attractors by using a piecewise-linear function. Boya et *al.,* introduce a novel six-scroll chaos and multistability into a simple Thomas system and use this complex behavior for medical data privacy [10]. Njitacke et al., used the heterogeneous structure of neuron models to express energy dissipation, infinite coexistence, selected control, and multi-scroll structures [11–14]. Kengne et *al.,* explored the coupling of some systems and displayed complex coexisting states and multi-scroll attractors based on coupling schemes [15–18].

Some complex schemes of formation of multi-scrolls have been shown by using Hopfield Neural Networks with various structures of rich structures. Lin et *al.,* [19] revealed rich n-scroll chaotic attractors from a memristive magnetized Hopfield neural network. Zhang et *al.* [20], investigated an offset boosting coexisting attractors with multi-double-scrolls in a memristive Hopfield neural network. Similarly, Bao et *al.* [21], revealed rich plane coexisting dynamics with two memristor-based Hopfield neural networks (HNNs). Yu et *al.,* found multi-scrolls in multiple directions and coexistence of multiple double-scroll chaos within a memristive HNN under considerations of external disturbance [22]. Tang et *al.* [23], investigated the dynamical analysis of memristive HNNs based on a multi-segment function and revealed hyperchaotic multi-scrolls.

The study of chaotic dynamics in coupled neurons has attracted much attention in recent years due to its potential applications in neuroscience and engineering [24]. In this context, the concept of multi-scroll chaos has emerged as a useful tool for modeling complex behavior in neural systems. Yu et *al.*, reveal rich complex bursting oscillations and synchronization phenomena issues through a memristive neural network [25]. Madasamy et *al.,* [26] studied the bidirectional coupling of two Hopfield inertial neurons with monotonic and non-monotonic activation functions and uncovered chameleon dynamics with elegant multi-scroll chaos formation. Some recent works show that artificial neural networks under different activation functions reveal rich dynamical behaviors in the brain, which are not observed when we have a single activation function [26,27]. Dongmo and Kengne [28] discussed a chain bidirectional coupling of four inertial systems revealing coexisting multi-stable patterns with the merging of multi-scroll chaos.

Non-oscillatory neurons exhibit complex dynamics that can lead to chaotic behavior. Investigating multi-scroll chaos in these systems enhances our understanding of how neural networks can display rich dynamical properties, which are crucial for modeling brain functions and understanding neurological disorders.

Understanding the mechanisms of multi-scroll chaos in coupled non-oscillatory neurons under different activation functions provides a more accurate representation of certain types of neural circuits found in the brain, particularly in regions where oscillatory behavior is not predominant. Moreover, it is an important area of research for both basic neuroscience and engineering applications. While it may offer benefits in terms of complexity and robustness, it also presents challenges to control and predictability.

In this paper, we will explore the complex dynamics of two coupled single-inertial Hopfield neurons owning two different monotonic activation functions. Thus, our objectives in this work are as follows.

- Propose a novel coupling of two non-oscillatory neurons with different monotonic activation functions;
- Present complex coexistence of multi-scroll chaos with their corresponding phase space magnetization through basins of attraction;
- Display the bursting oscillation present in this model;
- Control the multistable behavior of multiple double-scrolls using time feedback control and show the desired one at the end of the control;
- Finally, propose the microcontroller implementation of the model.

The layout of the paper is as follows: Section II discusses the mathematical model and basic properties of the bidirectional coupling model. Section III presents investigations highlighting complex activities in the proposed model and focuses on the time feedback of the desired multi-scroll. Section IV presents the microcontroller realization of the model. Finally, the last section concludes the paper.

2. Theoretical investigations

A. The coupling model

The primary focus of the study lies in coupled non-oscillatory neurons, neural models devoid of intrinsic oscillations but capable of exhibiting complex chaotic behavior when interconnected. By coupling two non-oscillating inertial neuron models constituted with different activation functions, we obtain the following system:

$$\begin{cases} \dot{x} = u \\ \dot{u} = -\varepsilon u - (x + \alpha y) + c_1 f_1(x + \alpha y) \\ \dot{y} = v \\ \dot{v} = -\varepsilon v - (y + \beta x) + c_2 f_2(y + \beta x) \end{cases} \tag{1}$$

where c_1, c_2 represent the synapse of the neurons. ε describes the inertial term of the neuron; α and β are coupling parameters. $f_1(w) = \tanh(w)$, $f_2(w) = \arcsin h(w)$ describe the activation functions of the first and second neurons, respectively. By scrutinizing the collective dynamics of these neurons with different coupled activation functions, we aim to unveil the underlying mechanisms of complex behaviors of interconnected networks.

B. Equilibrium points and stability

The equilibrium points of the coupled neurons (1) are calculated by setting all derivatives to zero. After solving, we obtain nine equilibrium points described as follows:

$$E_0\begin{pmatrix}0\\0\\0\\0\end{pmatrix}, E_{1,2}\begin{pmatrix}\pm\theta_1\alpha\eta\\0\\\mp\theta_1\eta\\0\end{pmatrix}, E_{3,4}\begin{pmatrix}\pm\theta_1\eta\\0\\\mp\theta_1\beta\eta\\0\end{pmatrix}, E_{5,6}\begin{pmatrix}\pm\eta(\theta_1-\alpha\theta_2)\\0\\\pm\eta(\theta_2-\beta\theta_1)\\0\end{pmatrix}, E_{7,8}\begin{pmatrix}\pm\eta(\theta_1+\alpha\theta_2)\\0\\\mp\eta(\theta_2+\beta\theta_1)\\0\end{pmatrix} \text{ with } \eta=(1-\alpha\beta)^{-1}.$$

$\theta_1 = x+\alpha y$, and $\theta_2 = y+\beta x$. By replacing θ_1 and θ_2 in Eq. (1) we will obtain the numerical values of these parameters by fixing the values of the synapses.

The linear perturbation of system (1) is gives the Jacobian matrix described in Eq. (2),

$$M=\begin{bmatrix}0 & 1 & 0 & 0\\ \phi_1(\theta_1)-\varepsilon & \alpha\,\phi_1(\theta_1) & 0\\ 0 & 0 & 0 & 1\\ \beta\phi_2(\theta_2) & 0 & \phi_2(\theta_2)-\varepsilon\end{bmatrix} \tag{2}$$

with $\phi_1(\theta_1)=c_1\left(1-tan\,h^2(\theta_1)\right)-1$ and $\phi_2(\theta_2) = c_2/\left(\sqrt{(\theta_2)^2+1}\right)-1$.

Eq. (2) above are used to discuss the stability of any equilibrium points through the Routh Hurwitz criterion. The characteristic equation associated to this model (1) as follows

$$p(\lambda)=\lambda^4+\delta_3\lambda^3+\delta_2\lambda^2+\delta_1\lambda^1+\delta_0 \tag{3}$$

Where $\delta_k(k=0,1,2,3)$ represent the coefficient of the characteristic equation. These coefficient are given in Table 1 according to each equilibrium point with their related stabilities.

From the data presented in Table 1, the first five equilibrium points are always unstable due to these with coefficients of the characteristic polynomial equation with different signs. The four other equilibrium points involve conditional stability due to the parameters of the model. This implies that Hopf bifurcation occurs in this model. The critical value ε_c related to the transition from a stable state to an oscillatory state from the above equilibrium points is given by eq. (4).

$$\varepsilon_c=\sqrt{-w_c^2+(1-\alpha\beta)\frac{2\left(-1+c_1\left(1-tan\,h^2(\theta_1)\right)\right)\left(-1+c_2\Big/\left(\sqrt{(\theta_2)^2+1}\right)\right)}{w_c^{-2}}} \tag{4}$$

The frequency of stable oscillations and the non-degeneracy condition have been obtained respectively by eqs. (5) and (6).

Table 1
The equilibrium points of model (1) and their stabilities.

Equilibrium points	Coefficient of the characteristic equation (3)	Stability
$E_0\begin{pmatrix}0\\0\\0\\0\end{pmatrix}$	$\begin{bmatrix}\delta_3=2\varepsilon\\ \delta_2=\varepsilon^2+2-c_1-c_2\\ \delta_1=\varepsilon(2-c_1-c_2)\\ \delta_0=(1-\alpha\beta)(-1+c_1)(-1+c_2)\end{bmatrix}$	Unstable
$E_{1,2}\begin{pmatrix}\pm\theta_2\alpha\eta\\0\\\mp\theta_2\eta\\0\end{pmatrix}$	$\begin{bmatrix}\delta_3=2\varepsilon\\ \delta_2=\varepsilon^2+2-c_1-c_2/\left(\sqrt{(\theta_2)^2+1}\right)\\ \delta_1=\varepsilon\left(2-c_1-c_2/\left(\sqrt{(\theta_2)^2+1}\right)\right)\\ \delta_0=(1-\alpha\beta)(-1+c_1)\left(-1+c_2/\left(\sqrt{(\theta_2)^2+1}\right)\right)\end{bmatrix}$	Unstable
$E_{3,4}\begin{pmatrix}\pm\theta_1\eta\\0\\\mp\theta_1\beta\eta\\0\end{pmatrix}$	$\begin{bmatrix}\delta_3=2\varepsilon\\ \delta_2=\varepsilon^2+2-c_1\left(1-tan\,h^2(\theta_1)\right)-c_2\\ \delta_1=\varepsilon\left(2-c_1\left(1-tan\,h^2(\theta_1)\right)-c_2\right)\\ \delta_0=(1-\alpha\beta)\left(-1+c_1\left(1-tan\,h^2(\theta_1)\right)\right)(-1+c_2)\end{bmatrix}$	Unstable
$E_{5,6}\begin{pmatrix}\pm\eta(\theta_1-\alpha\theta_2)\\0\\\pm\eta(\theta_2-\beta\theta_1)\\0\end{pmatrix}$; $E_{7,8}\begin{pmatrix}\pm\eta(\theta_1+\alpha\theta_2)\\0\\\mp\eta(\theta_2+\beta\theta_1)\\0\end{pmatrix}$	$\begin{bmatrix}\delta_3=2\varepsilon\\ \delta_2=\varepsilon^2+2-c_1\left(1-tan\,h^2(\theta_1)\right)-c_2/\left(\sqrt{(\theta_2)^2+1}\right)\\ \delta_1=\varepsilon\left(2-c_1\left(1-tan\,h^2(\theta_1)\right)-c_2/\left(\sqrt{(\theta_2)^2+1}\right)\right)\\ \delta_0=(1-\alpha\beta)\left(-1+c_1\left(1-tan\,h^2(\theta_1)\right)\right)\left(-1+c_2/\left(\sqrt{(\theta_2)^2+1}\right)\right)\end{bmatrix}$	Conditional stability

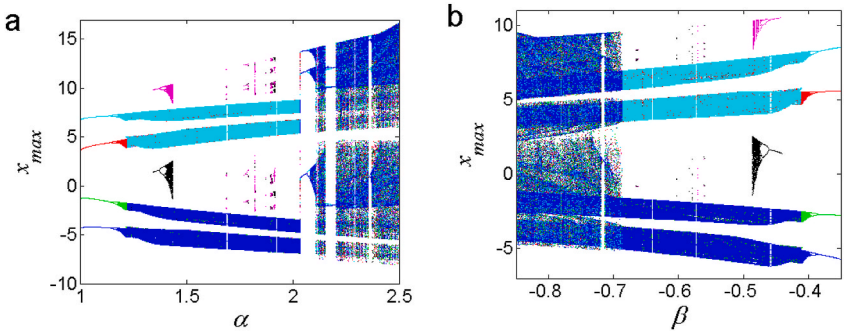

Fig. 1. Bifurcation diagram displaying the evolution of periodic to chaotic motion, when monitoring α in $\alpha \in [1,\ 2.5]$ *with* $\beta = -0.48$ (a) *and* β *in* $\beta \in [-0.85,\ -0.35]$, *with* $\alpha = 1.42$ (b). *Other parameters are set* $\varepsilon = 0.56, c_1 = 2.4, c_2 = 2.4$.

$$w_c = \sqrt{-0.5\left(-2 + c_1\left(1 - tan\, h^2(\theta_1)\right) + c_2 \Big/ \left(\sqrt{(\theta_2)^2 + 1}\right)\right)} \tag{5}$$

$$Real\left(\frac{d\lambda}{d\varepsilon_c}|_{\varepsilon=\varepsilon_c}\right) = \frac{-2w_c^2}{\varepsilon_c^2 + 4w_c^2} \neq 0 \tag{6}$$

Thus, the model presents self-excited attractors for a specific parameter range.

3. Numerical investigation

In this section, numerical analysis is performed using nonlinear analysis tools with the high precision of the fourth-order Runge-Kutta algorithm to conduct the dynamics analysis of the pairing of two non-oscillatory neurons.

1. Dynamic behavior

The present model with two different activation functions reveals an elegant formation of multi-scroll chaos, justified by the coexistence of four bifurcation diagrams with two parallel branch bifurcation diagrams. Fig. 1 shows the complex structure of four-scroll chaos according to some specific values of coupling parameters. In Fig. 1(a), the dynamical evolution of α shown in the range $\alpha \in [1;\ 2.5]$ when other parameters are fixed $\varepsilon = 0.56, c_1 = 2.4, c_2 = 2.4$ and $\beta = -0.48$ under initial conditions $(\pm 1, 0, 0, 0)$ computed in upward and downward directions with fixed values. Similarly, β undergoes a reversal from periodic to chaotic multi-scroll in the range $\beta \in [-0.85,\ -0.35]$, with $\alpha = 1.42$, $\varepsilon = 0.56$, $c_1 = 2.4$, and $c_2 = 2.4$, with the same initial conditions as provieded in Fig. 1(b). The Lyapunov spectrum corresponding to these bifurcation diagrams is provided in Fig. 2(a)–(b). From Fig. 2, it can be seen that there is a maximum of one positive Lyapunov exponents in some regions, while in others, there are all negatives. Thus, these coupling neurons present periodic and chaotic behaviors.

According to Fig. 1(a), some striking phase portraits are present in the plane (x, y) describing the road to four-scroll chaos formation. In Fig. 3(a), the model shows coexistence between two double-scroll chaos with one pair of single-scroll chaos obtained when

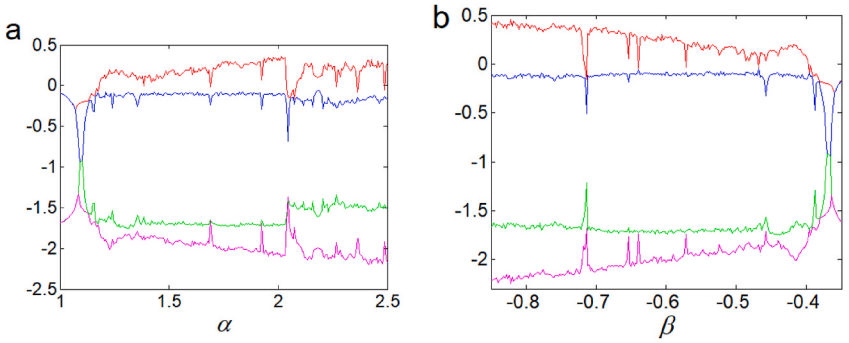

Fig. 2. (a)–(b) Lyapunov spectrum corresponding to Fig. 1(a)–(b).

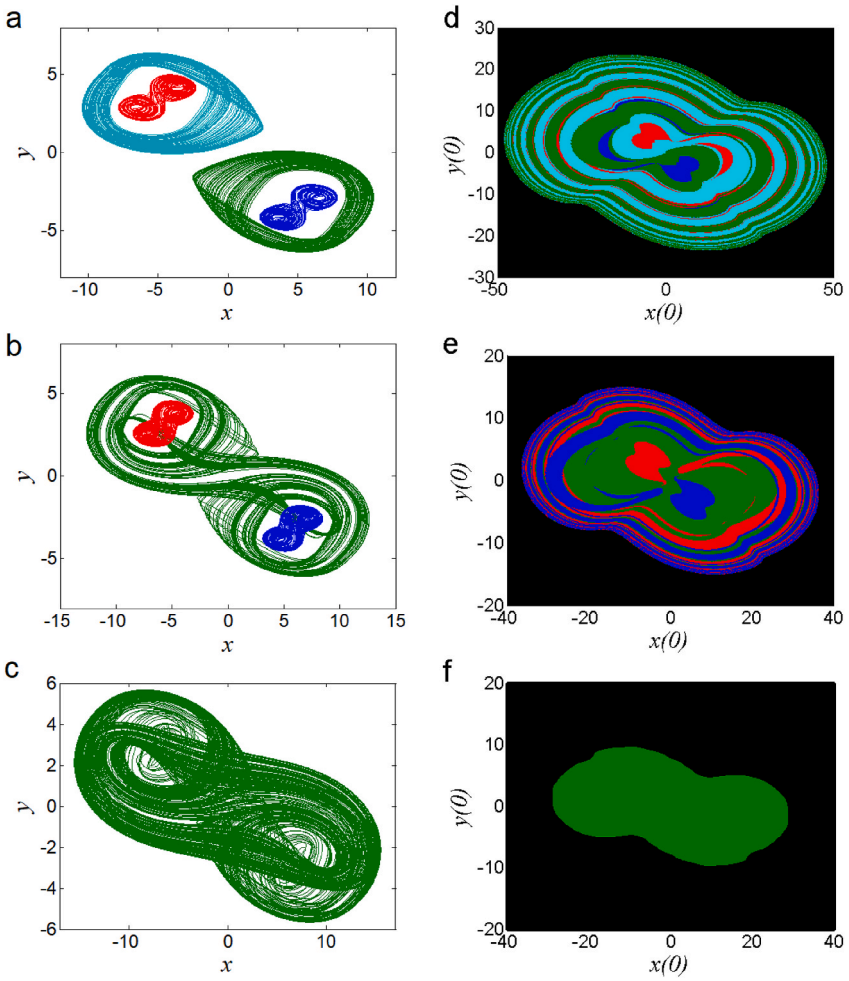

Fig. 3. (a)–(c) Phase portraits plotted in the plane (x,y) and (d)–(f) basins of attraction plotted in the plane $(x(0),y(0))$ *showing the coexisting road to four scroll − chaos formation.* (*a*) *Coexistence between two double − scroll chaos with one pair of single scroll − chaos at* $\alpha = 1.435$ *with initial conditions* $(0,0,\pm 1,0)$, *and* $(0,0,\pm 2,0)$, (*b*) *coexistence of three double − scroll chaotic attractors coexisting at* $\alpha = 1.822$ *with initial conditions* $(0,-1,1,1)$ and $(\pm 2, -1,1,1)$, (*c*) *formation of four scroll chaotic attractor at* $\alpha = 2.4$ *with initial conditions* $(0,0,1,0)$. In the basins of attraction, black color indicates unbounded oscillations and others colors correspond to each coexisting attractors.

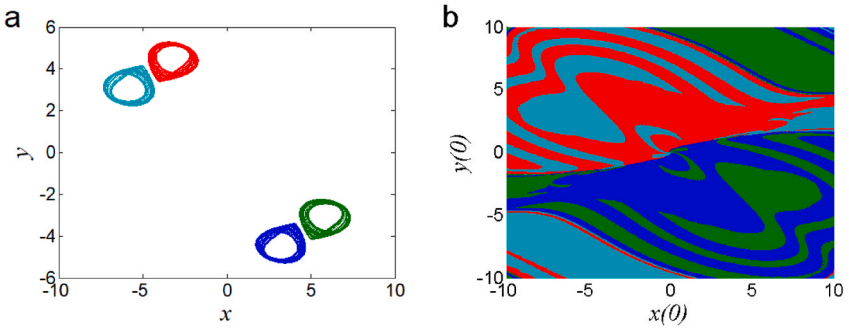

Fig. 4. (a) Phase portraits plotted in the plane (x,y) and (b) cross section of the basins of attraction plotted in the plane $(x(0), y(0))$ *showing the coexistence of four single − scroll chaos when* $\alpha = 1.2$ *with initial conditions* $(0,0,\pm 1,0)$, and $(0,0,\pm 4,0)$. Color of the cross sections of the basins of attraction correspond to each coexisting attractors.

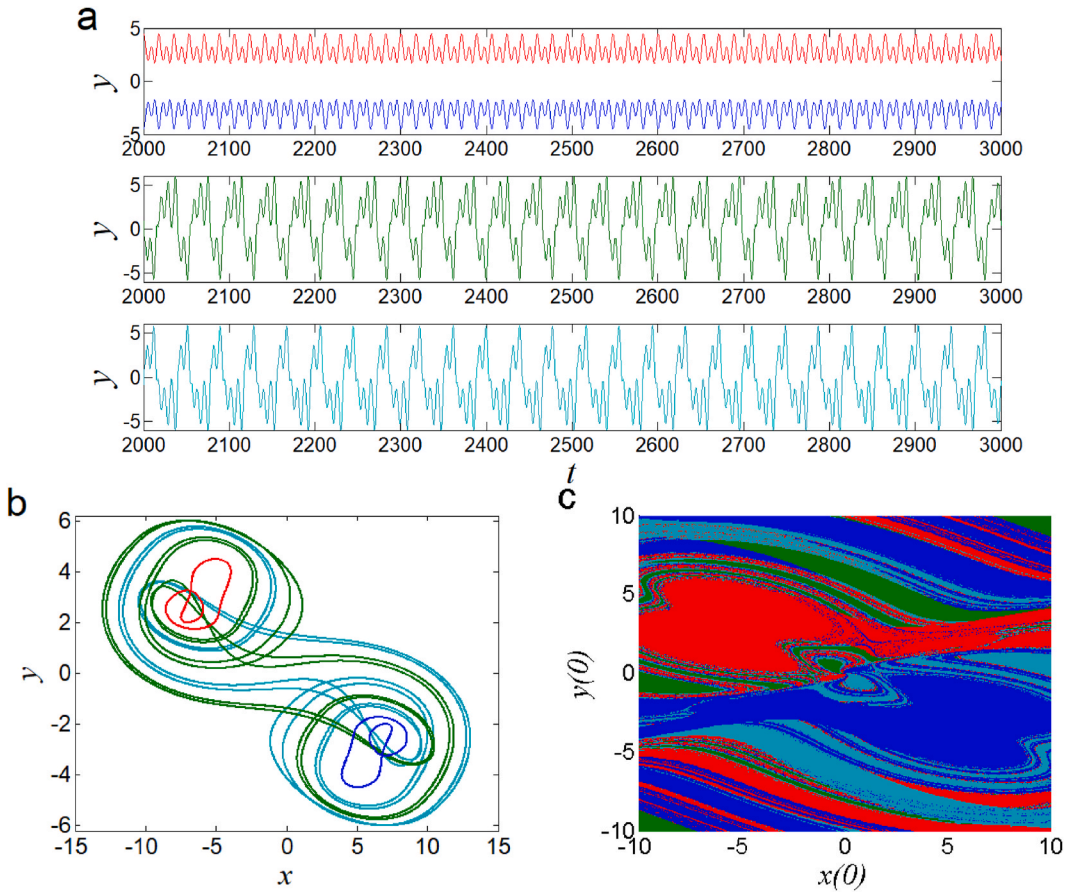

Fig. 5. (a) Time-domain waveforms plotted in the plane (t, y), (b) *phase portraits plotted in the plane* (x, y) and (c) cross section of the basins of attraction plotted in the plane $(x(0), y(0))$ *displaying the coexistence of four periodic spiking bursting partners for* $\alpha = 1.896$ *with initial conditions* $(0, 0, \pm 1, 0)$, *and* $(0, 0, \pm 3.9, 0)$. Color of the cross sections of the basins of attraction correspond to each coexisting attractors.

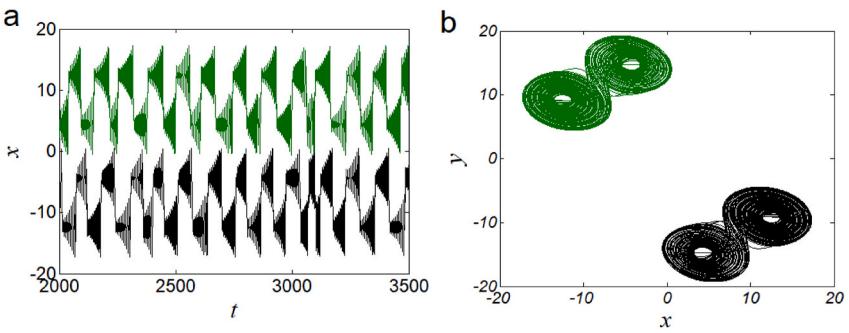

Fig. 6. (a) Time-domain waveforms plotted in the plane (t, x), *and* (b) *involving the coexistence of symmetric bursting partners when parameters are set as*, $\varepsilon = 0.56, c_1 = 6, c_2 = 5, \alpha = 0.7$ *and* $\beta = -0.7$ *under initial conditions* $(\pm 1, 0, 0, 0)$.

$\alpha = 1.435$ under initial conditions $(0, 0, \pm 1, 0)$, and $(0, 0, \pm 2, 0)$. The pair of single-scrolls merge into a single double-scroll chaos and coexist with a pair of two other double-scroll chaos when $\alpha = 1.822$ with initial conditions $(0, -1, 1, 1)$ and $(\pm 2, -1, 1, 1)$ as shown in Fig. 3(b). The formation of the four-scroll chaotic attractor is presented in Fig. 3(c) when $\alpha = 2.4$ with initial conditions $(0, 0, 1, 0)$. In the basins of attraction, the black color indicates unbounded oscillations and other colors correspond to each coexisting attractor (please see Fig. 3(d)–(f)).

Some complex oscillations of multistability are discussed in this work. Multistability is a phenomenon that presents the coexistence of multiple solutions for the same parameter values under different initial conditions [29–32].

Multistability refers to a phenomenon in which a system can exist in multiple stable states or configurations under the same set of conditions. Multistability is an interesting property of neural dynamics [33], which appears in forced, coupled, and self-reproducing systems [34–37]. It holds significance in image encryption as well [38]. In Fig. 4(a), a fascinating result is showcased, revealing the presence of four homogeneous strange attractors when $\alpha = 1.2$ under specific initial conditions $(0,0,\pm 1,0)$, and $(0,0,\pm 4,0)$. The plot illustrates these attractors in the plane (x,y), along with a cross-section of the basins of attraction depicted in the plane $(x(0),y(0))$. Each coexisting attractor is color-coded for clarity, as shown in Fig. 4(b). Furthermore, the coupling model discussed in this work explores the spiking multistability of four periodic spiking oscillations, comprising a pair of period-2 cycles and a pair of period-4 cycles. These oscillations manifest when $\alpha = 1.896$ given specific initial conditions $(0, 0, \pm 1, 0)$, and $(0, 0, \pm 3.9, 0)$. The complex spiking oscillations are visually represented through time-domain waveforms in the plane (t,y), phase portraits plotted in the plane (x, y), and cross-sections of the basins of attraction in plane $(x(0),y(0))$, as depicted in Fig. 5(a)–(c) respectively.

2. Bursting oscillations

Bursting oscillations are a type of dynamic behavior observed in various biological and artificial systems, characterized by the occurrence of rapid bursts of activity followed by periods of quiescence or slower oscillations. These oscillations can be described as a sequence of spikes or rapid oscillatory events that occur in clusters, separated by intervals of relative inactivity. Bursting oscillations play a crucial role in signal processing and communication within the brain. They allow for the rapid transmission of information in a synchronized manner, which is important for functions such as sensory perception, motor control, and cognitive processes [39–41]. In addition, bursting activity can help regulate the overall excitability of neural networks, influencing the likelihood of generating action potentials in response to incoming signals. This complex activity is present in this model when parameters are set as $\varepsilon = 0.56$, $c_1 = 6$, $c_2 = 5$, $\alpha = 0.7$ and $\beta = -0.7$ and initial conditions $(\pm 1,0,0,0)$. Fig. 6(a) displays the waveforms of chaotic bursting oscillation plotted in the plane (t,x), it corresponding phase portraits plotted in the plane (x,y) (see Fig. 6(b)).

3. Control of multistability

The feedback term method in control theory involves adding a space-dependent feedback term to the dynamical equations of a system to guide the dynamics toward a desired attractor by suppressing other attractors. This method is particularly effective in controlling multistability, where multiple attractors coexist in chaotic systems. The magnitude of the feedback is adjusted based on the difference between a state variable and an unstable fixed point near the desired attractor. Unlike the linear increase control method commonly used for managing multistability [32], the feedback term approach is simpler and does not require expanding the system's size. Increasing the system's size can alter the dynamics and affect the coexisting attractors during control. With the feedback term method, the control is initiated by selecting a specific attractor as the "designated survivor attractor," providing predictability in the outcome of the control process.

The temporal feedback control method is explored in this paper to enable one to target any desired state, for an initial time only and inactive afterward. In order to exploit the temporal feedback method introduced by Ref. [42], and define as follows:

$$\dot{X} = F(x) - \zeta h(t)(X - \lambda) \tag{7}$$

where X is the m-dimensional vector of dynamical variables for the nonlinear system and $F(x)$ is a vector field describing its dynamics. ζ is the feedback strength, λ represent the parameter of desired attractor and the time dependent term $h(t)$ can be defined as,

$$h(t) = \begin{cases} 1 & if \quad t \le t_{\min} + \tau \\ 0 & if \quad otherwise \end{cases} \tag{8}$$

where $t_{\min}$ represents the transient regime while τ is a pulse of some duration. Therefore, the controlled neurons are given as follow,

$$\begin{cases} \dot{x} = u - h(t)\,\zeta(x - \lambda) \\ \dot{u} = -\varepsilon u - (x + \alpha y) + c_1 f_1(x + \alpha y) \\ \dot{y} = v \\ \dot{v} = -\varepsilon v - (y + \beta x) + c_2 f_2(y + \beta x) \end{cases} \tag{9}$$

By carefully choosing the space-dependent term and adjusting the feedback strength, the undesired attractors gradually converge toward the designated survivor attractor. The control of the coexistence of the three double-scroll chaos of Fig. 3(b) is carried out in Fig. 7(a) when $\lambda = 0.3$ for double-scroll chaos in green color and in Fig. 8(a) when, and $\lambda = 6$ for double-scroll chaos in blue color.

During these controls, we can see that the other double-scroll chaotic attractors gradually converge to the designated survivor attractors with the increase in the feedback strength ζ when $\tau = 5$. In Figs. 7 (b) and Fig. 8 (b), these phase portraits of the attractors at the end of the control process demonstrate that the attractors align with the designated survivor attractors with the same color. This outcome confirms the effectiveness of the feedback term method in controlling neural system with multiple attractors. Moreover, this method offers practical advantages for applications as it allows for targeted control of specific attractors without uncertainty about the final outcome, unlike other control methods that may not guarantee a specific attractor after control is applied.

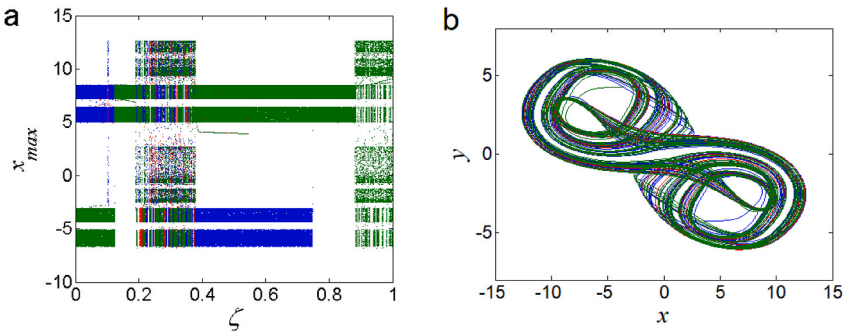

Fig. 7. (a) Bifurcation diagrams illustrating the unselected trajectory of Fig. 3 (b) merge with the one of the desired trajectory when the control parameter of coupling strength ζ of the controlled system and phase portrait of the chaotic desired attractor obtained when $\zeta = 1$ (b). *These diagrams are obtained for* $\varepsilon = 0.56, c_1 = 2.4, c_2 = 2.4,\ \alpha = 1.822, \beta = -0.48, \tau = 5,$ and $\lambda = 0.3$.

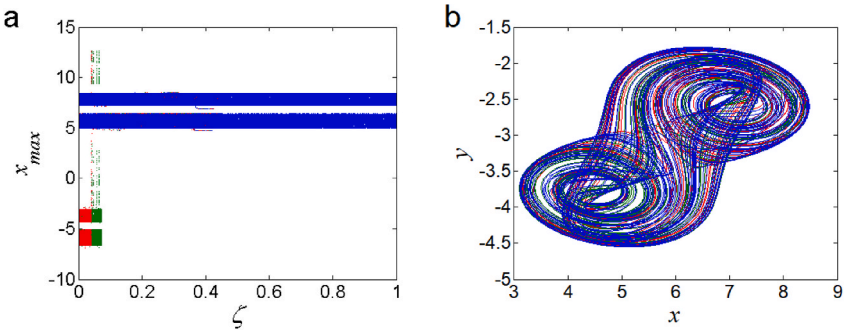

Fig. 8. (a) Bifurcation diagrams illustrating the unselected trajectory of Fig. 3 (b) merge with the one of the desired trajectory when the control parameter of coupling strength ζ of the controlled system and phase portrait of the chaotic desired attractor obtained when $\zeta = 1$ (b). *These diagrams are obtained for* $\varepsilon = 0.56, c_1 = 2.4, c_2 = 2.4,\ \alpha = 1.822, \beta = -0.48, \tau = 5,$ and $\lambda = 6$.

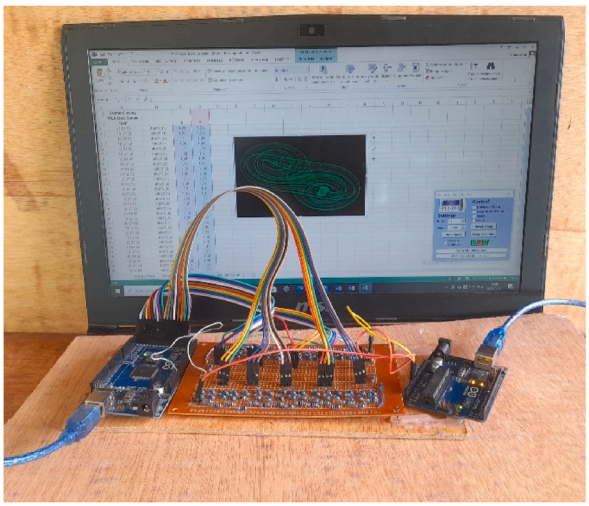

Fig. 9. Experimental setup of the microcontroller-based realization displaying the four-scroll chaos plotted in the plane (x, y), obtained with same parameters of Fig. 3 (c).

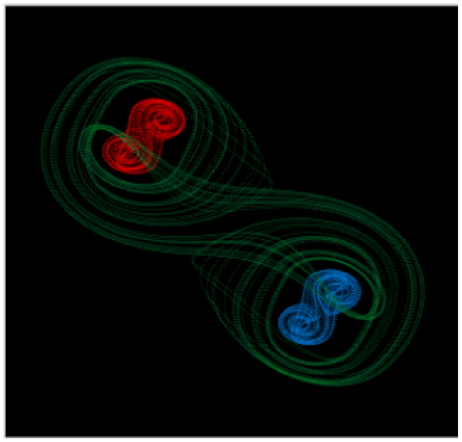

Fig. 10. Microcontroller-based realization showing the coexistence of three double scroll chaotic attractors plotted in the plane (x,y).

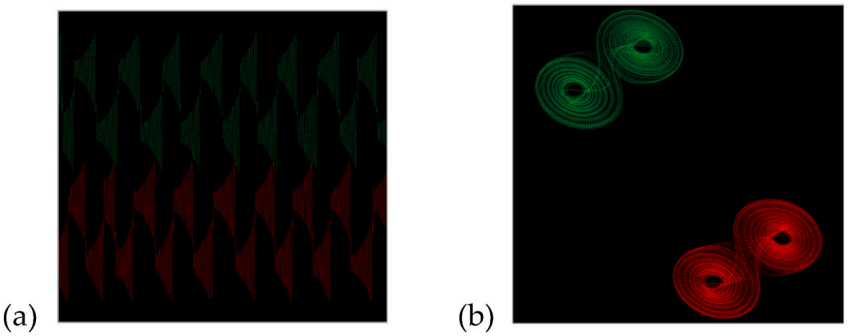

Fig. 11. Microcontroller-based realization showing the coexistence of chaotic bursting partners. (a) Time series plotted in the plane (t, x), *and* (b) *phase portrait plotted in the plane* (x,y), obtained with same parameters of Fig. 6.

4. Microcontroller-based realization

The microcontroller hardware platform offers a reliable alternative to analog circuit experiments, which are susceptible to errors due to parasitic parameters and temperature drift. By using the digital circuit method described in literature [43–45], we perform the microcontroller realization of the proposed coupling bi-neuron model. The experimental setup of the microcontroller-based implementation is shown in Fig. 9, where we can observe the four-volute chaos drawn in the plane (x,y). The Arduino Mega Board is used here as a digital calculator, and the Arduino Uno is used for real-time data acquisition. A 16-bit digital-to-analog converter is used in this experiment to convert the digital data into analog signals.

The model parameters used in Figs. 3(b) and 6 were maintained for these experiments, ensuring consistency in the comparison of results between numerical and microcontroller implementation (respectively present in Figs. 10 and 11(a)–(b)). Figs. 10–11 further illustrates the experimental outcomes achieved through the microcontroller implementation, showcasing the effectiveness and reliability of this approach in studying complex dynamical systems like the coupled Hopfield inertial neurons.

5. Conclusion

This study successfully demonstrates the existence of a family of coexisting multi-scroll chaos in a network of coupled non-oscillatory Hopfield neurons. Through a comprehensive analysis involving phase portraits, basins of attraction, time series, bifurcation diagrams, and Lyapunov exponents, it provides a comprehensive exploration of the complex dynamics inherent to this system. The coexistence of multiple bifurcation diagrams results in an intricate scheme of multi-scroll formation, further complicated by bursting oscillations and multiple firing partners. A control strategy utilizing a noninvasive method is effectively applied to select the desired multi-scroll. An experimental validation on an Arduino microcontroller is supported to verified numerical simulations. The selected control of desired attractors opens avenues for applications in various fields, including neural network design and medical data privacy. In particular, the ability to manipulate multi-scroll chaos could optimize the performance of the cryptosystems, enhancing data security.

CRediT authorship contribution statement

Bertrand Frederick Boui A Boya: Writing – review & editing, Writing – original draft, Validation, Software, Formal analysis, Conceptualization. **Zeric Tabekoueng Njitacke:** Writing – review & editing, Writing – original draft, Validation, Software, Formal analysis. **Adelaide Nicole Kengnou Telem:** Writing – review & editing, Writing – original draft, Software, Formal analysis, Conceptualization. **Jacques Kengne:** Writing – review & editing, Writing – original draft, Visualization, Software, Formal analysis, Conceptualization.

Ethical approval

Not applicable.

Data and code availability statement

No new data was generated for the research described in the article.

Declaration of competing interest

The authors declare the following financial interests/personal relationships which may be considered as potential competing interests:Bertrand Frederick BOUI A BOYA reports a relationship with University of Dschang that includes: non-financial support. If there are other authors, they declare that they have no known competing financial interests or personal relationships that could have appeared to influence the work reported in this paper.

References

[1] J. Ma, J. Tang, A review for dynamics in neuron and neuronal network, Nonlinear Dynam. 89 (2017) 1569–1578.
[2] H. Lin, C. Wang, Q. Deng, C. Xu, Z. Deng, C. Zhou, Review on chaotic dynamics of memristive neuron and neural network, Nonlinear Dynam. 106 (2021) 959–973.
[3] Q. Lai, L. Yang, G. Hu, Z.-H. Guan, H.H.-C. Iu, Constructing multiscroll memristive neural network with local activity memristor and application in image encryption, IEEE Trans. Cybern. 54 (2024) 4039–4048.
[4] S. Zhang, C. Chen, Y. Zhang, J. Cai, X. Wang, Z. Zeng, Multidirectional multidouble-scroll hopfield neural network with application to image encryption, IEEE Transactions on Systems, Man, and Cybernetics: Systems (2024).
[5] H. Bao, R. Ding, B. Chen, Q. Xu, B. Bao, Two-dimensional non-autonomous neuron model with parameter-controlled multi-scroll chaotic attractors, Chaos, Solit. Fractals 169 (2023) 11. Paper No. 113228.
[6] N. Wang, G. Zhang, H. Li, Parametric control for multi-scroll attractor generation via nested sine-PWL function, IEEE Transactions on Circuits and Systems II: Express Briefs 68 (2020) 1033–1037.
[7] Y. Yang, L. Huang, J. Xiang, Q. Guo, Three-dimensional sine chaotic system with multistability and multi-scroll attractor, IEEE Transactions on Circuits and Systems II: Express Briefs 69 (2021) 1792–1796.
[8] S.K. Dana, B.K. Singh, S. Chakraborty, R.C. Yadav, J. Kurths, G.V. Osipov, et al., Multiscroll in coupled double scroll type oscillators, International Journal of Bifurcation and Chaos 18 (2008) 2965–2980.
[9] J.L. Echenausía-Monroy, S. Jafari, G. Huerta-Cuéllar, H. Gilardi-Velázquez, Predicting the emergence of multistability in a Monoparametric PWL system, International Journal of Bifurcation and Chaos 32 (2022) 2250206.
[10] Boya, B.F. Boui A, A. Nanfak, M.N. Joseph, B.L. Klimentyevna, JdD. Nkapkop, J.Y. Effa, Six-scroll chaos within the dynamics of the Thomas chaotic system and application to biomedical data encryption, Phys. Scripta 100 (2024) 015244.
[11] Z.T. Njitacke, T.F. Fozin, S.S. Muni, J. Awrejcewicz, J. Kengne, Energy computation, infinitely coexisting patterns and their control from a Hindmarsh–Rose neuron with memristive autapse: circuit implementation, AEU-International Journal of Electronics and Communications 155 (2022) 154361.
[12] Z.T. Njitacke, J. Awrejcewicz, A.N.K. Telem, T.F. Fozin, J. Kengne, Complex dynamics of coupled neurons through a memristive synapse: extreme multistability and its control with selection of the desired state, IEEE Transactions on Circuits and Systems II: Express Briefs 70 (2022) 791–795.
[13] I.S. Doubla, B. Ramakrishnan, Z.N. Tabekoueng, J. Kengne, K. Rajagopal, Infinitely many coexisting hidden attractors in a new hyperbolic-type memristor-based HNN, Eur. Phys. J. Spec. Top. 231 (2022) 2371–2385.
[14] J. Ramadoss, C.N. Takembo, A. Karthikeyan, Z.T. Njitacke, J. Awrejcewicz, Effect of external excitation on the isolated and collective dynamics of a generic FitzHugh–Rinzel neuron, The European Physical Journal Plus 138 (2023) 1–10.
[15] S. Sriram, A.A. Danao, T.F. Fonzin, K. Rajagopal, J. Kengne, Coexistence of multiscroll chaotic attractors in two coupled inertial hopfield neurons: numerical simulations and experiment, Phys. Scripta 97 (2022) 125207.
[16] S. Balaraman, J. Kengne, M.K. Fogue, K. Rajagopal, From coexisting attractors to multi-spiral chaos in a ring of three coupled excitation-free Duffing oscillators, Chaos, Solit. Fractals 172 (2023) 113619.
[17] H.-D. Mekak-Egong, B. Ramakrishnan, A.N.K. Telem, K. Rajagopal, J. Kengne, Multiscroll in bidirectionally coupled jerk oscillators: theoretical analysis and PSpice verification, International Journal of Bifurcation and Chaos 32 (2022) 2250211.
[18] O.M. Njimah, J. Ramadoss, A.N.K. Telem, J. Kengne, K. Rajagopal, Coexisting oscillations and four-scroll chaotic attractors in a pair of coupled memristor-based Duffing oscillators: theoretical analysis and circuit simulation, Chaos, Solit. Fractals 166 (2023) 112983.
[19] H. Lin, C. Wang, Y. Sun, T. Wang, Generating n-scroll chaotic attractors from a memristor-based magnetized hopfield neural network, IEEE Transactions on Circuits and Systems II: Express Briefs 70 (2022) 311–315.
[20] S. Zhang, J. Zheng, X. Wang, Z. Zeng, S. He, Initial offset boosting coexisting attractors in memristive multi-double-scroll Hopfield neural network, Nonlinear Dynam. 102 (2020) 2821–2841.
[21] H. Bao, M. Hua, J. Ma, M. Chen, B. Bao, Offset-control plane coexisting behaviors in two-memristor-based Hopfield neural network, IEEE Trans. Ind. Electron. 70 (2022) 10526–10535.
[22] F. Yu, X. Kong, W. Yao, J. Zhang, S. Cai, H. Lin, et al., Dynamics analysis, synchronization and FPGA implementation of multiscroll Hopfield neural networks with non-polynomial memristor, Chaos, Solit. Fractals 179 (2024) 114440.
[23] D. Tang, C. Wang, H. Lin, F. Yu, Dynamics analysis and hardware implementation of multi-scroll hyperchaotic hidden attractors based on locally active memristive Hopfield neural network, Nonlinear Dynam. 112 (2024) 1511–1527.
[24] P.C. Matthews, R.E. Mirollo, S.H. Strogatz, Dynamics of a large system of coupled nonlinear oscillators, Phys. Nonlinear Phenom. 52 (1991) 293–331.

[25] X. Yu, H. Bao, Q. Xu, M. Chen, B. Bao, Deep brain stimulation and lag synchronization in a memristive two-neuron network, Neural Network. 180 (2024) 106728.
[26] E. Madasamy, B.F.B. a Boya, J. Kengne, K. Rajagopal, Collective dynamics of two coupled Hopfield inertial neurons with different activation functions: theoretical study and microcontroller implementation, Phys. Scripta 98 (2023) 095219.
[27] Q. Deng, C. Wang, H. Lin, Memristive Hopfield neural network dynamics with heterogeneous activation functions and its application, Chaos, Solit. Fractals 178 (2024) 114387.
[28] T.N. Sogui Dongmo, J. Kengne, Multiple scroll attractors and multistability in the collective dynamics of a four chain coupled Hopfield inertial neuron network: analysis and circuit design investigations, Phys. Scripta 99 (2024) 065223.
[29] C. Hens, S.K. Dana, U. Feudel, Extreme multistability: attractor manipulation and robustness, Chaos: An Interdisciplinary Journal of Nonlinear Science 25 (2015) 053112.
[30] G.D. Leutcho, S. Jafari, I.I. Hamarash, J. Kengne, Z.T. Njitacke, I. Hussain, A new megastable nonlinear oscillator with infinite attractors, Chaos, Solit. Fractals 134 (2020) 109703.
[31] M.I. Tametang Meli, G.D. Leutcho, D. Yemele, Multistability analysis and nonlinear vibration for generator set in series hybrid electric vehicle through electromechanical coupling, Chaos: An Interdisciplinary Journal of Nonlinear Science 31 (2021).
[32] A.N. Pisarchik, U. Feudel, Control of multistability, Phys. Rep. 540 (2014) 167–218.
[33] P. Heyward, M. Ennis, A. Keller, M.T. Shipley, Membrane bistability in olfactory bulb mitral cells, J. Neurosci. 21 (2001) 5311–5320.
[34] J.S. Kelso, Multistability and metastability: understanding dynamic coordination in the brain, Phil. Trans. Biol. Sci. 367 (2012) 906–918.
[35] H. Lin, C. Wang, Y. Sun, W. Yao, Firing multistability in a locally active memristive neuron model, Nonlinear Dynam. 100 (2020) 3667–3683.
[36] Q. Xu, Y. Wang, B. Chen, Z. Li, N. Wang, Firing pattern in a memristive Hodgkin–Huxley circuit: numerical simulation and analog circuit validation, Chaos, Solit. Fractals 172 (2023) 113627.
[37] B.F.B.A. Boya, J. Kengne, G.D. Kenmoe, J.Y. Effa, Four-scroll attractor on the dynamics of a novel Hopfield neural network based on bi-neurons without bias current, Heliyon 8 (2022) e11046.
[38] S. Zhang, J. Zheng, X. Wang, Z. Zeng, A novel no-equilibrium HR neuron model with hidden homogeneous extreme multistability, Chaos, Solit. Fractals 145 (2021) 110761.
[39] F. Zeldenrust, W.J. Wadman, B. Englitz, Neural coding with bursts—current state and future perspectives, Front. Comput. Neurosci. 12 (2018) 48.
[40] A. Schnitzler, J. Gross, Normal and pathological oscillatory communication in the brain, Nat. Rev. Neurosci. 6 (2005) 285–296.
[41] C.W. Lynn, D.S. Bassett, The physics of brain network structure, function and control, Nature Reviews Physics 1 (2019) 318–332.
[42] K. Yadav, A. Prasad, M.D. Shrimali, Control of coexisting attractors via temporal feedback, Phys. Lett. 382 (2018) 2127–2132.
[43] B.F.B.A. Boya, B. Ramakrishnan, J.Y. Effa, J. Kengne, K. Rajagopal, The effects of symmetry breaking on the dynamics of an inertial neural system with a non-monotonic activation function: theoretical study, asymmetric multistability and experimental investigation, Phys. Stat. Mech. Appl. 602 (2022) 127458.
[44] R. Balamurali, A.N.K. Telem, J. Kengne, K. Rajagopal, M-e Hermann-Dior, On the mechanism of multiscroll chaos generation in coupled non-oscillatory Rayleigh-duffing oscillators, Phys. Scripta 97 (2022) 105207.
[45] J.B. Koinfo, S. Sriram, K. Jacques, A. Karthikeyan, Investigation on the regular and chaotic dynamics of a ring network of five inertial Hopfield neural network: theoretical, analog and microcontroller simulation, Cognitive Neurodynamics (2024) 1–27.